NANO LETTERS

Letter

pubs.acs.org/NanoLett

Selective and Sensitive Sensing of Flame Retardant Chemicals Through Phage Display Discovered Recognition Peptide

Hyo-Eon Jin,[†,§] Chris Zueger,[‡,§] Woo-Jae Chung,[†,§] Winnie Wong,[†,§] Byung Yang Lee,[*,†,§,∥] and Seung-Wuk Lee[*,†,§]

[†]Department of Bioengineering and [‡]Department of Mechanical Engineering, University of California, Berkeley, California 94720, United States

[§]Physical Biosciences Division, Lawrence Berkeley National Laboratory, Berkeley, California 94720, United States

[∥]Department of Mechanical Engineering, Korea University, Seoul 136-713, Korea

S *Supporting Information*

ABSTRACT: We report a highly selective and sensitive biosensor for the detection of an environmentally toxic molecule, decabrominated diphenyl ether (DBDE), one of the most common congeners of the polybrominated frame retardants (polybrominated diphenyl ether (PBDE)), using newly discovered DBDE peptide receptors integrated with carbon nanotube field-effect transistors (CNT-FET). The specific DBDE peptide receptor was identified using a high-throughput screening process of phage library display. The resulting binding peptide carries an interesting consensus binding pocket with two Trp-His/Asn-Trp repeats, which binds to the DBDE in a multivalent manner. We integrated the novel DBDE binding peptide onto the CNT-FET using polydiacetylene coating materials linked through cysteine-maleimide click chemistry. The resulting biosensor could detect the desired DBDE selectively with a 1 fM detection limit. Our combined approaches of selective receptor discovery, material nanocoating through click chemistry, and integration onto a sensitive CNT-FET electronic sensor for desired target chemicals will pave the way toward the rapid development of portable and easy-to-use biosensors for desired chemicals to protect our health and environment.

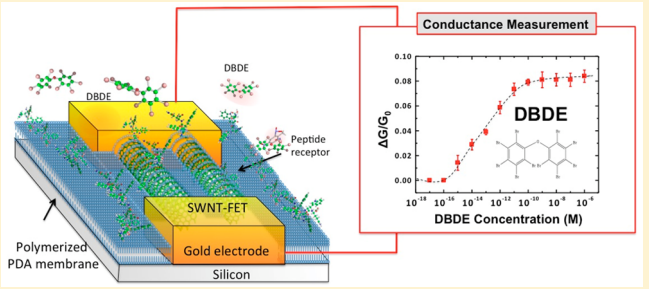

KEYWORDS: *Phage display, polybrominated diphenyl ether, environmental toxicant, biosensor*

Polybrominated diphenyl ethers (PBDEs) are environmentally toxic chemicals that have been utilized worldwide for many decades as flame retardant additives in a large number of products such as plastics in electronics and computers, upholstery, and furniture foams.[1−3] Covalent bonds between carbon−bromine in the PBDEs can be easily broken through thermal stimulation to generate bromine radicals, which prevent flame propagation by intercepting carbon radicals.[4] However, the PBDEs are not chemically fixed to the final products; they are slowly released over the life of the products and can seriously contaminate environments.[5,6] PBDEs are highly lipophilic so they are easily accumulated in fat tissues.[7] In addition, PBDEs have long estimated half-lives reaching up to 12 years in the human body.[8] Therefore, the bioaccumulation in the human body causes serious health effects, especially for infants and pregnant women.[2,9,10] Furthermore, there are more than 200 different kinds of congeners of PBDEs that possess different health effects.[11] Therefore, the ability to accurately detect various PBDEs in the environment is increasingly important. However, current PBDE measurement can only be accomplished with expensive laboratory equipment and complex procedures such as chromatography-based mass-spectrometry methods and spectroscopy, which have limited use for early detection.[12−14] PBDE binding behaviors against proteins and various substrates have been previously studied; crystallographic studies of the estrogen sulfotransferase with PBDEs have shown that rich phenylalanine and tyrosine residues are present on the active binding site of PBDEs.[15] Computational calculations also showed that small changes of the bromine sites of the PBDEs greatly affected the $\pi-\pi$ interaction between the PBDEs and substrates.[16] Despite previous studies on the structure dependent binding between PBDE and desired substrates, it has been very challenging to develop a specific receptor for the PBDEs because of their low solubility in aqueous solutions and the similarity of the 200 congener structures. Therefore, the receptor based sensor development for PBDEs is still in its infancy. Thanks to the advent of biotechnology, we can mimic the evolution process of Mother Nature through the recombinant design of a basic building block of life (i.e., nucleic acids and amino acids).

Received: September 11, 2015
Revised: October 6, 2015

DOI: 10.1021/acs.nanolett.5b03678
Nano Lett. XXXX, XXX, XXX−XXX

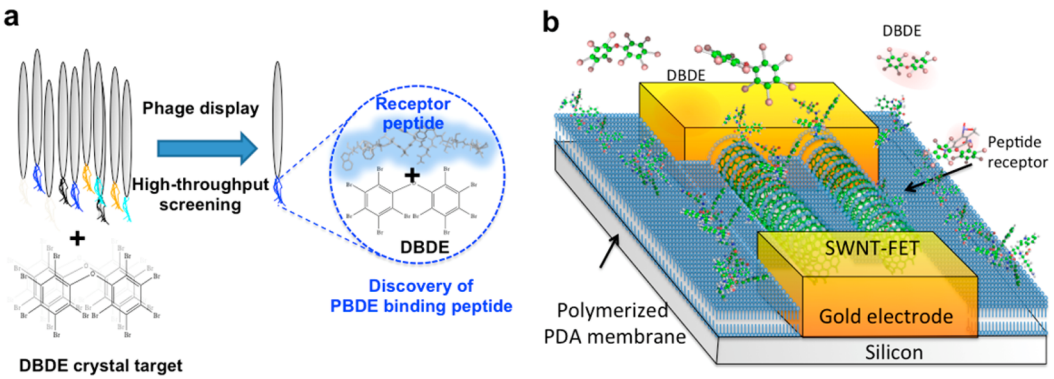

Figure 1. Schematic illustration of the DBDE binding peptide discovery through phage display (a) and integration of the DBDE binding peptides on the CNT-FET (b).

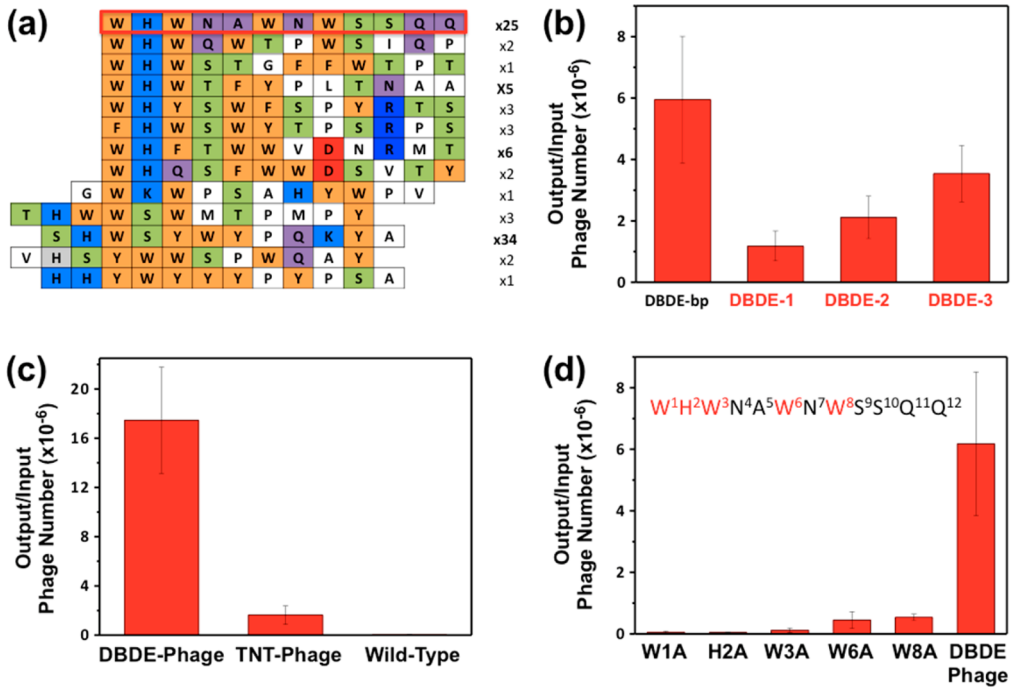

Figure 2. Discovery of DBDE binding peptides and their binding characterization. (a) Collection of phage display results with the consensus binding peptide sequences (WHW). Different amino acids were labeled as follow: Aromatic residue (orange); positively charged residue (blue), negatively charged residue (red); hydroxylated residue (green), hydrophobic side chain (white). Competitive binding assay results shown in the right column. Red box indicates the DBDE binding peptide. (b) Comparative binding studies of the DBDE-bp (WHWNAWNWSSQQ), DBDE-1 (SHWSYWYPQKYA), DBDE-2 (WHFTWWVDNRMT), DBDE-3 (WHWTFYPLTNAA). (c) Comparison of the binding affinity for DBDE among DBDE binding phage (DBDE-phage, WHWNAWNWSSQQ) and TNT binding phage (TNT-phage, WHWQRPLMPVSI), Wild-type phage (Wild-type, no insert). (d) Comparison binding assay results among alanine substitution assays for the first Trp to Ala (W1A), the second His to Ala (H2A), the third Trp to Ala (W3A), the sixth Trp to Ala (W6A), and the eighth Trp to Ala (W8A) from the DBDE-phage. The insert 12-mer DBDE-bp sequence was displayed. The mutation sites were colored in red.

Specifically, phage display and Systematic Evolution of Ligands by EXponential enrichment (SELEX) have been excellent high-throughput screening processes for discovering novel peptides or DNA/RNA aptamers that bind to relevant chemicals for biosensors, such as pesticides, explosives, and antigens.[17−19] Therefore, identification of specific receptors for the PBDEs and their integration on the sensitive transducers may be the next step toward developing sensitive and selective biosensors for the PBDEs. Here, we report a highly selective and sensitive biosensor to detect decabrominated diphenyl ether (DBDE), one of the highly utilized PBDE congeners, through the development of specific binding peptides for DBDE and their integration on sensitive carbon nanotube field-effect transistors (CNT-FET) (Figure 1). We utilized a biomimetic high-throughput screening process, phage library display, to identify specific peptide-based receptors for the DBDE. We then integrated the DBDE receptor onto a CNT-FET electronic sensor using polydiacetylene based nanocoating materials, interfacing the selective DBDE binding event to sensitive electric signal generation. We demonstrated that the resulting electronic sensor possessed excellent selectivity for the target DBDE with a detection limit of 1 fM level. It can specifically discriminate many different similar chemicals of the PBDEs. Our receptor-based sensor development approach for the desired target chemicals provides an excellent pathway for the

DOI: 10.1021/acs.nanolett.5b03678
Nano Lett. XXXX, XXX, XXX−XXX

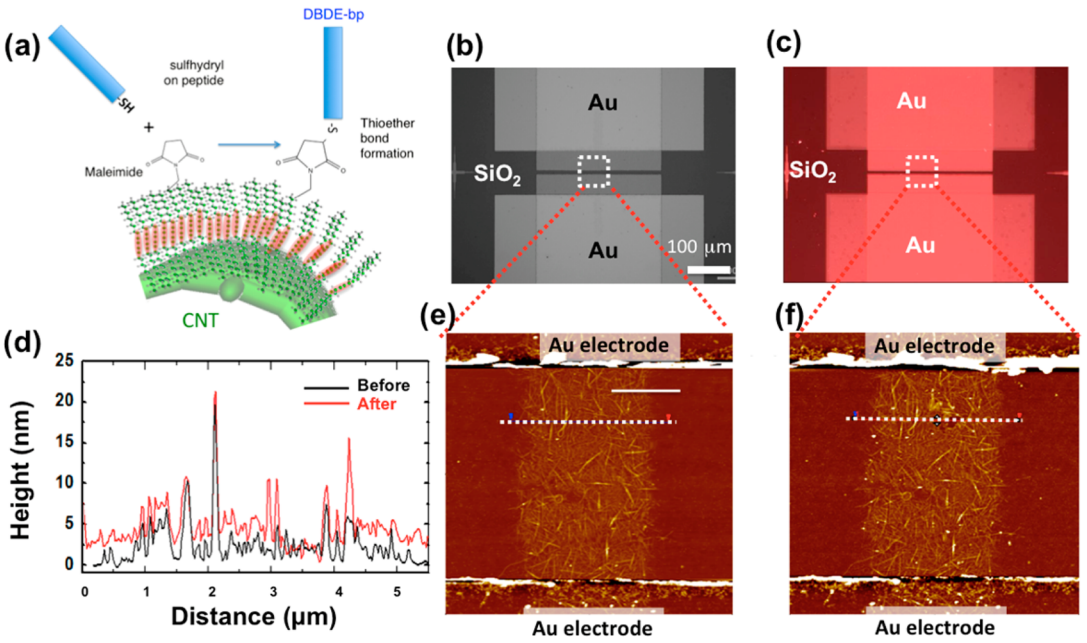

Figure 3. Fabrication of the PDA nanocoating layers on the CNT-FET. (a) Schematic illustration of the DBDE-bp conjugated polydiacetylene nanocoating layers on the top of the CNT-FET. Microscopy images of the CNT-FET devices before (b) and after (c) the application of the DBDE-bp nanocoating layers. After application of the PDA coating layers, we could observe the red fluorescence signal from the devices. (d) Atomic force microscopy cross-sectional height profile analyses from the CNT-FET devices before and after the application of the PDA coating layers. AFM images of the CNT-FET before (e) and after the PDA coating layer application (f).

rapid development of portable and easy-to-use detectors of harmful toxicants in the environment to protect human health.

Results and Discussion. The specific DBDE-binding peptide was identified by biomimetic evolutionary screening process of phage library display (details in Supporting Information). In short, we prepared a crystal form of DBDE compounds through recrystallization processes to prepare homogeneous target substrates. We then applied a 12-mer phage peptide library (~10^{11} pfu) onto the DBDE crystals, and followed repetitive washing steps to remove weakly binding or nonbinding peptide carrying phage. The bound phage was recovered with pH elution buffer (HCl-Gly buffer at pH 2.2) and enriched through amplification in bacterial host cells. The enriched phage library was applied to DBDE crystals with increased stringency induced by increased TWEEN 20 surfactant concentrations. After three rounds of the selection process, we randomly picked phages and sequenced their DNA to discover the DBDE-binding peptides (DBDE-bp). We performed two independent sets of the phage display screening process (see the results in Table S1 in the Supporting Information). We observed that after four rounds of screening, the DBDE binding sequences were narrowed down to a consensus peptide motif that carries multiple aromatic binding pockets (Figure 2a). This consensus motif contains consistently spaced groups of amino acids with nonpolar aromatic (tryptophan and phenylalanine) and polar (tyrosine) aromatic side chains at the N terminus of the receptor. Interestingly, there are aromatic−aromatic or aromatic−X−aromatic binding pockets in nearly all the sequences, indicating that $\pi-\pi$ interactions play a major role in the binding events. Similar trends have been previously shown to bind selectively to the explosive molecules (i.e., trinitrotoluene (TNT)).[20] We prepared a mini-library of the DBDE binding phages carrying aromatic-rich consensus binding peptide. We then performed an additional round of the competitive binding phage selection against the DBDE crystals. Through random selection, we identified the top four highly binding candidates for the DBDE (Figure 2a). We then performed the comparative binding assay: The amount of bound phage (output concentration with respect to the input phage concentration) was quantified for each type of phage (Figure 2b). Through binding assays, the sequence **WHW**NA**W**N**W**SSQQ (**Trp**-His-**Trp**-Asn-Ala-**Trp**-Asn-**Trp**-Ser-Ser-Gln-Gln), which we will refer to as the DBDE-binding peptide, was identified as the best binding peptide for DBDE. Previous work demonstrated the active site of the PBDE interacting proteins, estrogen sulfotransferase, was associated with multiple aromatic amino acid residues upon binding with PBDEs.[15] Prominent binding sequences representing several variations in the spacing of the aromatic side chains were compared in a binding assay to determine their relative binding affinity under identical conditions. Similarly, the affinity of the DBDE binding phage was compared to the previously discovered TNT binding phage and unmodified wild type phage (Figure 2c). The TNT binding phage has the binding motif of WHW[20] and a very similar N-terminal region to the DBDE-bp. However, we observed that the phage with the DBDE binding sequence had a much higher binding affinity toward DBDE compared to the TNT binding phage. This means the peptide sequence outside WHW of the DBDE-bp plays an important role in the selective and multivalent binding of the DBDE-bp toward DBDE. The wild type phage showed relatively negligible binding affinity toward the DBDE. In order to verify the presumed importance of the aromatic side chain containing amino acids within the DBDE peptide binding sequence, an alanine substitution mutation assay was conducted (detailed procedures in Supporting Information). Each of the four tryptophans and the histidine were individually substituted with the alanine as an alanine-scanning test.[17,21] The alanine substitution mutation assay results (Figure 2d) showed that each alanine substitution caused a large decrease in the binding

DOI: 10.1021/acs.nanolett.5b03678
Nano Lett. XXXX, XXX, XXX−XXX

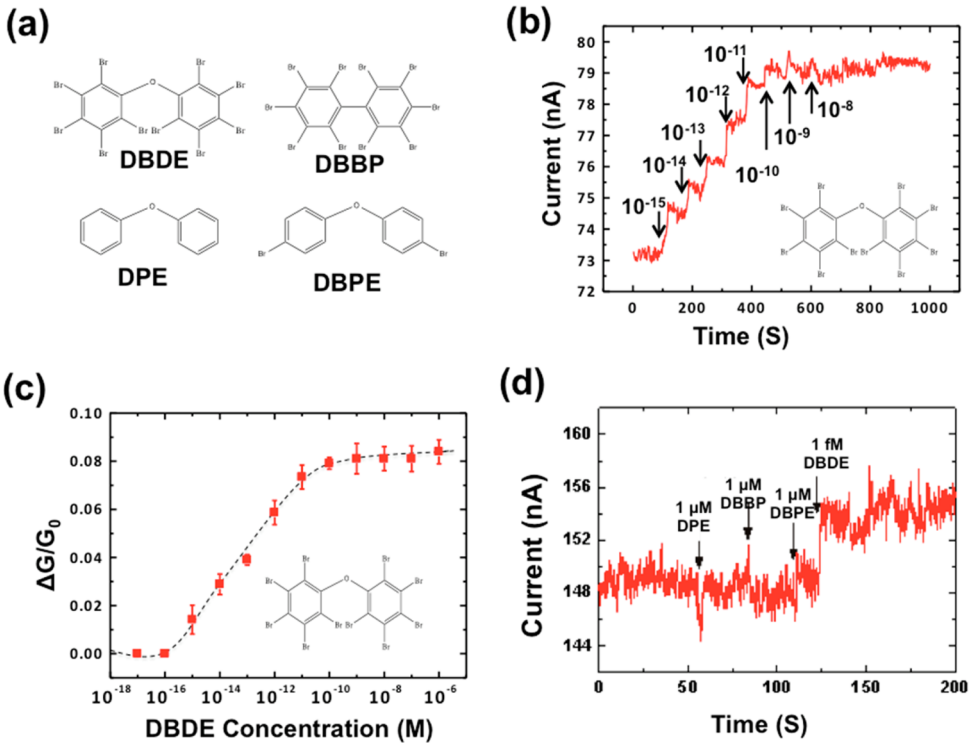

Figure 4. Sensitive and selective detection of the DBDE using DBDE-binding peptide imbedded CNT-FET. (a) Chemical structure of DBDE, DBBP, DPE, and DBPE. (b) Sensitive detection of the DBDE on current measurement between source and drain of CNT-FET. (c) Standard curves for the DBDE detection calibrated. (d) Selectivity of the DBDE sensor against other chemicals possessing similar chemical structures to the DBDE, such as DPE, DBBP, and DBPE.

affinity of that particular phage with respect to the original DBDE binding phage. Substitution of the tryptophan residues nearest the N-terminus of the pIII protein caused the greatest change in binding affinity, while substitution of those closest to the C-terminus resulted in a smaller though still substantial change. Along with the lower binding affinity of the TNT binding sequence, this result demonstrates that the DBDE-bp bound to the target DBDE through a sequence specific manner and the entire sequence is important for the selective binding to DBDE.

We integrated the identified DBDE recognition peptides onto a CNT-FET electronic sensor platform after confirmation of the DBDE binding peptide affinity.[22,23] We previously showed that polydiacetylene can effectively interface the peptide receptor binding events with the conductance signal generation of the CNT-FET.[22] By following the established protocol, we integrated the PDA membrane onto the CNT-FET. Our CNT-FET consisted of source and drain electrodes connected by a CNT network assembled on a silicon substrate. The CNT network was composed of single and bundled CNTs, which resulted in a combination of semiconducting and metallic paths. In the CNT network, the semiconducting CNTs contributed to the current change from external chemical stimuli. However, the metallic or bundled CNTs formed metallic electrical paths that were not affected by external stimuli. The basic electronic properties of the CNT-FET showed a typical resistance value of 0.5−2 MΩ, and an on−off ratio of ∼4 in air (Supporting Information Figure S1). The CNT-FET was first coated with a lipid-like polydiacetylene (PDA) membrane by applying 5 μL of PDA solution. Illumination of UV light (365 nm wavelength) polymerized the diacetylene backbone, making the CNT-FET devices capable of transducing chemical environmental changes. In order to link the DBDE binding peptide, we included the 4% maleimide group as a versatile chemical handle for thioether bond formation. Using this chemical handle, any peptide linked to Cys can be conveniently integrated to the CNT-FET devices. Therefore, we synthesized the DBDE binding peptide terminated with the Cys and linked DBDE-bp with the CNT-FET (Figure 3a).[22,24] The successful coating process was verified by observing the fluorescence microscopy and atomic force microscopy characterization before and after the application of the PDA coating layer.[25] Figure 3b,c shows the fluorescence microscopy characterization before and after the PDA coating layer application. After the illumination of UV light, the device showed fluorescent emission (Figure 3c). Atomic force microscopy (AFM) characterization of the CNT-FET also confirmed the uniform integration of the PDA coating layers. AFM height profile measurement (Figure 3d) from the cross-section on top of the CNT-FET (dotted line in Figure 3e,f) showed that the thickness increased ∼2 nm on average after application of the PDA layers. We thoroughly tested the resulting devices before the DBDE sensing characterization. The liquid gate characteristics were observed to verify the effectiveness of our PDA coating without DBDE peptide as a passive layer. The liquid gate characteristics of uncoated pristine CNT-FET were observed before and after DBDE injection. As shown in Supporting Information Figure S2, the CNT-FET showed a right-ward shift in the $I-V_g$ characteristics because the DBDE molecules are directly adsorbed on the CNT surface, p-doping the CNTs by the electronegative bromines in the DBDE molecules.[26] A proper PDA coating should keep the DBDE molecules from directly interacting with the CNTs and only through the DBDE-bp receptors. The

DOI: 10.1021/acs.nanolett.5b03678
Nano Lett. XXXX, XXX, XXX−XXX

effectiveness of the PDA coating was verified by coating the CNT-FET with PDA/PDA-maleimide without DBDE-bp receptors and then introducing DBDE molecules. As shown in Supporting Information Figure S3, when the CNT-FET was coated with the PDA/PDA-maleimide coating layer, the gate transfer characteristics did not change significantly. This indicates that the PDA without DBDE binding peptides can passivate the CNT-FET successfully and demonstrates the effectiveness of the coating process.

We functionalized the PDA/PDA-maleimide coated CNT-FET with the DBDE-bp using maleimide-thioether click chemistry, where the thiol in the cysteine-terminating DBDE-bp (at C-terminal) and the maleimide group formed the thioether bond (Figure 3a).[27] We then applied the DBDE and various similar chemicals to the DBDE (Figure 4a) to the DBDE-bp receptor functionalized CNT-FET sensor. In order to characterize the detection limit of the biosensor, which we defined as the lowest concentration at which the sensor shows a detectable response signal, we applied various dilutions of DBDE in a mixture of PBS buffer and acetonitrile (1:1 v/v) into the sensing system starting from 100 aM to higher concentrations. The sensor began to exhibit a noticeable electric sensing signal from a 1 fM solution. This detection limit (Figure 4b) corresponds to ∼0.001 ng/L in w/v concentration, which is 2 orders of magnitude lower compared to GC-MS based techniques.[28,29] The current increase in Figure 4b can be explained by the chemical gating effects of DBDE binding to DBDE-bp anchored to the PDA layer with signal amplification through the conjugated PDA which induced additional positive charges in the CNTs, thus increasing the conductance of p-type CNTs.[22] The sensor response, defined as the ratio of conductance change ΔG to initial conductance G_0, showed saturation above 0.1 nM. Through the application of the variously diluted solutions, we obtained the standard curves (Figure 4c). The dynamic range, defined as the range of target concentration at which the sensor shows a significant sensing signal response, of the DBDE receptor functionalized sensor showed a wide value of 10^{-15} to 10^{-8} M. The effect of the receptor was verified by observing the sensor response in the absence of DBDE-bp (Supporting Information Figure S4). The sensor showed little response to 1 nM and 1 μM DBDE in the absence of DBDE-bp. Finally, selectivity tests were performed toward other molecules with similar chemical structures to DBDE (Figure 4a,d), such as diphenyl ether (DPE), decabromobiphenyl (DBBP), and DBPE (a PBDE congener with two bromines). DBPE is known as one of other abundant PBDE congeners in the United States.[30] Figure 4d shows the real-time response when 1 μM of DPE, DBBP, and DBPE were injected. The sensor showed little response to DPE and DBBP, and only little interference to DBPE, showing that the sensor is sensitive to the existence of the ether group, and the number of bromines. This excellent selectivity can be explained by the multivalent binding nature of the DBDE-bp against the DBDE. A feasible mechanism of the molecular recognition is the interaction of two aromatic binding pockets (WHW and WNW) of the DBDE-bp with the aromatic rings of the DBDE molecule. In addition, complementary charge−charge interactions between electropositive histidine and electronegative oxygen and bromine in the DBDE molecule further contribute the multivalent binding between DBDE-bp and DBDE. We believe that this multivalent binding interaction is also responsible for the large difference in affinity between DBDE-bp and TNT-binding sequence shown in Figure 2c. Finally, these binding events can affect the electronic density of the DBDE-bp conjugated PDA electronic backbone, which can be detected by the CNT-FET within the vicinity of ∼2 nm from the PDA-conjugated backbone, as shown in Figure 3d. A similar sensing signal response was observed in our previous CNT-FET devices coated with PDA layer conjugated with TNT binding peptides.[22]

In conclusion, we demonstrated a highly selective and sensitive DBDE sensor by combining the newly discovered DBDE-binding peptide receptor, a PDA-based lipid-like molecular coating layer, and highly sensitive CNT-FETs. Through the biomimetic high-throughput phage peptide screening process, we discovered a novel consensus binding peptide for DBDE. The DBDE receptor incorporated with CNT-FET sensor was able to detect down to 1 fM concentration of DBDE with little interference from other congeners of PBDE or other chemically similar molecules. Our chemoselective thioether bond formation-based receptor functionalization method is versatile enough to easily functionalize the CNT-FET-coated PDA with other receptors. For future practical applications, further studies will be performed in other selective receptors for PBDE congeners and miniaturization of the sensors. Our combined approaches to integrate discovery of the peptide with sensitive electronic sensors will pave the way for the rapid development of useful, portable and low-cost environment monitoring systems to protect human health.

Materials and Methods. *Materials.* Ph.D.-12, Phage Display Peptide Library Kits were purchased from New England Biolabs (Ipswich, MA). Tris-HCl, Glycine-HCl, NaCl, BSA, Tween-20, and IPTG/X-gal were purchased from Sigma-Aldrich (St. Louis, MO). Carbon nanotubes were obtained from Hanhwa Co. (Seoul, Korea). For peptide synthesis, Rink Amide resin, 3-maleimidopropionic acid and Fmoc-amino-acids were purchased from Novabiochem (San Diego, CA). Trifluoroacetic acid, thioanisole, phenol, ethanedithiol, 1,8-diazabicyclo[5.4.0]undec-7-ene (DBU), *N*,*N*′-diisopropylcarbodiimide (DIC), tri-isopropyl silane, 2-[2-(Fmoc-amino)ethoxy]ethoxy}acetic acid, and 10,12-pentacosadiynoic acid (PCDA) were obtained from Sigma-Aldrich (St. Louis, MO).

Phage Display. 12-mer phage peptide library (10^{11} pfu/μL) was applied to a crystal form of the DBDE grown through recrystallization processes. The DBDE crystals were incubated with the phage library and washed ten times with washing buffer to remove weakly binding or nonbinding phages. The bound phage was recovered with pH elution buffer (HCl-Gly buffer at pH 2.2) and enriched through amplification in bacterial host cells. The enriched phage library was applied to DBDE crystals with increased stringency induced by increased TWEEN 20 surfactant concentrations. After three rounds of selection processes, we identified the resultant DNA sequences to discover the dominant DBDE-binding peptide (DBDE-bp).

Comparative Binding Assay. We prepared a mini-library of the DBDE binding phages carrying aromatic-rich consensus binding peptide. We then performed an additional round of the competitive binding phage selection against the DBDE crystals. Through random selection, we identified the top four highly binding candidates for the DBDE. We then performed the comparative binding assay: The amount of bound phage (output concentration with respect to the input phage concentration) was quantified for each type of phage. In order to perform an alanine-scanning mutation binding assay,

DOI: 10.1021/acs.nanolett.5b03678
Nano Lett. XXXX, XXX, XXX−XXX

each of the four tryptophan amino acids and the histidine amino acid were individually substituted with the amino acid alanine that contains a small, symmetric, uncharged side chain. The mixture of equal amounts of the genetically modified alanine-substituted phages was panned against crystalline DBDE in the same way as the previous binding assays.

Maleimide-OEG-K-PDA Conjugate Synthesis. To produce PDA-maleimide conjugates, standard solid-phase peptide synthesis was carried out using Fmoc chemistry. Rink Amide resins were preswelled for 30 min in NMP prior to deprotection. Deprotection steps using 3 mL of 3% DBU in NMP were carried out for 20 min on a rocking platform. The washing steps proceeded as follows: three washes with 4 mL NMP, six washes with the series of 4 mL methanol followed by 4 mL dichloromethane, and three washes with 4 mL NMP. For all the coupling reactions, building blocks DIC and HOBt (5 equiv each) were mixed in NMP (~0.1 M for each component) and reacted with the resins (2 h). Complete coupling was confirmed by the Kaiser ninhydrin test. After deprotection of Fmoc groups on the resin, Fmoc-Lys(Mtt) was coupled to the resin and dried under vacuum. Mtt protecting group was cleaved with 4% TFA and 2.5% TIS in dichloromethane for 10 min. The resins were neutralized with 5% DIEA in DCM. Next, 10,12-pentacosadiynoic acid (PCDA) (5 equiv) was coupled to the α-amino group. Coupling of 2-[2-(Fmoc-amino)ethoxy]-ethoxy}acetic acid and 3-maleimidopropionic acid followed using the standard condition. After complete coupling, the resins were washed with dichloromethane, dried, and underwent cleavage. Cleavage reactions were performed for 2 h while shaking with a cocktail of 95% trifluoroacetic acid, 2.5% water, and 2.5% triisopropylsilane. Rotary evaporation followed by precipitation in diethyl ether removed the cleavage solvents and protecting groups. Samples were then suspended and mixed in water followed by centrifugation for 10 min at 10 000 rpm to pellet the product at which point the supernatant was discarded to remove any trace contaminants. The suspension and centrifugation steps were repeated until all cleavage contaminants were removed. Lyophilization was then performed and samples were stored at 4 °C. Cysteine-terminated DBDE-binding peptide was also synthesized using the standard Fmoc-chemistry-based solid-phase peptide synthesis described above. Cleavage reactions for the peptides were performed for 2 h while shaking with a cocktail of 82.5% trifluoroacetic acid, 5% water, 5% phenol, 5% thioanisole, and 2.5% ethanedithiol. Molecular weight of the synthesized peptide was confirmed using liquid chromatography mass spectrometer (LC-MS) before constructing the target vesicles (data not shown).

Fabrication of CNT-FET. The SiO_2 substrate was molecularly patterned with octadecyltrichlorosilane (OTS) self-assembled monolayer (SAM) using photolithography. Then, a single layer of single-walled CNTs was selectively adsorbed onto bare SiO_2 regions when the patterned substrate was dipped into the solution of single-walled CNTs (0.1 mg/mL in o-dichlorobenzene). Finally, electrodes (30 nm Au on 5 nm Cr) were fabricated via thermal evaporation and lift-off process. The fabricated CNT-FETs were characterized by measuring their *IV*-curves between source and drain electrodes and their initial resistance distribution. The CNT-FET showed quite linear *IV* characteristics. The slight nonlinearity is presumably due to the Schottky contacts between the semiconducting CNTs and the metal contacts (Supporting Information Figure S1). The back gating properties were measured for the CNT-FETs in air (Supporting Information Figure S2). The back gate voltage was swept from −10 to 10 V and the source-drain voltage was measured using Keithley 4200 semiconductor parameter analyzer. The CNT-FETs showed a typical p-type channel transistor response. The on−off ratio (the ratio to the on-current to the off-current) was about ~4.

CNT-FET Functionalization Process. The CNT-FET transducer was coated with a combination of polydiacetilene (PDA) and maleimide-functinalized PDA (maleimide-OEG-K-PDA) with the ratio of PDA/maleimide-OEG-K-PDA (96 mol % versus 4 mol % ratio). The ratio between PDA and maleimide-PDA was chosen according to our previous study, where this ratio resulted in optimum sensing for the target molecules (DBDE) and efficient signal transduction.[17,20,22] First, 10 mM PDA and maleimide-functionalized PDA were suspended in 96 mol % versus 4 mol % ratio in water. When solutions were incubated on the SWNT-FET surface, a lipid layer formed spontaneously via vesicle rupture and fusion. Polymerization was carried out for 25 min of exposure using a 4 W UV lamp at 254 nm wavelength. Afterward, the cysteine-terminating DBDE-bp in PBS/acetonitrile (1:1 v/v) was applied to the polymerized PDA/maleimide-PDA layer for 12 h to covalently anchor the DBDE-bp on the PDA/maleimide-functionalized PDA coat layer through thioether bond formation.

PBDE Sensing Experiments Using PBDE-bp-Coated CNT-FETs. The sensor response to the target PBDE and other interfering molecules was monitored in real time with a Keithley 4200 semiconductor parameter analyzer by observing the source-drain current of PBDE-bp-coated CNT-FETs in response to the addition of target analytes at a concentration range between 1 fM to 100 μM in PBS/acetonitrile (1:1 v/v) solution. A fluid cell was formed around the CNT-FET regions to confine the liquid during the experiment. A 50 μL PBS/acetonitrile (1:1 v/v) solution was applied first and then subsequent target analytes were injected. The source-drain voltage was kept at V_{ds} = 0.01 V, and a platinum liquid gate was kept at ground potential. Then, specific amounts of the target analyte solutions with different concentrations were subsequently added while monitoring the current level changes via the semiconductor parameter analyzer.

■ ASSOCIATED CONTENT

Supporting Information

The Supporting Information is available free of charge on the ACS Publications website at DOI: 10.1021/acs.nanolett.5b03678.

Additional figures of CNT-FET devices, characteristics of CNT-FETs and SWNT-FETs, as well as tables of phage results. (PDF)

■ AUTHOR INFORMATION

Corresponding Authors

*E-mail: (S.-W.L.) leesw@berkeley.edu
*E-mail: (B.Y.L.) blee@korea.ac.kr

Notes

The authors declare no competing financial interest.

■ ACKNOWLEDGMENTS

This work was supported by Center of Integrated Nanomechanical Systems (COINS) of the National Science Foundation (Grant EEC-0832819). B.Y.L. acknowledges the support from the National Research Foundation (NRF) funded

DOI: 10.1021/acs.nanolett.5b03678
Nano Lett. XXXX, XXX, XXX−XXX

by the Korea government (MSIP) (Grants 2015R1A2A2A04002733 and 2013R1A1A1010802).

REFERENCES

(1) Alaee, M.; Arias, P.; Sjödin, A.; Bergman, Å. *Environ. Int.* **2003**, *29*, 683.
(2) Frederiksen, M.; Vorkamp, K.; Thomsen, M.; Knudsen, L. E. *Int. J. Hyg. Environ. Health* **2009**, *212*, 109.
(3) Rahman, F.; Langford, K. H.; Scrimshaw, M. D.; Lester, J. N. *Sci. Total Environ.* **2001**, *275*, 1.
(4) Siddiqi, M. A.; Laessig, R. H.; Reed, K. D. *Clin. Med. Res.* **2003**, *1*, 281.
(5) Allchin, C. R.; Law, R. J.; Morris, S. *Environ. Pollut.* **1999**, *105*, 197.
(6) Jones-Otazo, H. A.; Clarke, J. P.; Diamond, M. L.; Archbold, J. A.; Ferguson, G.; Harner, T.; Richardson, G. M.; Ryan, J. J.; Wilford, B. *Environ. Sci. Technol.* **2005**, *39*, 5121.
(7) Siddiqi, M. A.; Laessig, R. H.; Reed, K. D. *Clin. Med. Res.* **2003**, *1*, 281.
(8) Vonmeyerinck, L.; Hufnagel, B.; Schmoldt, A.; Benthe, H. F. *Toxicology* **1990**, *61*, 259.
(9) She, J.; Holden, A.; Sharp, M.; Tanner, M.; Williams-Derry, C.; Hooper, K. *Chemosphere* **2007**, *67*, S307.
(10) Chevrier, J.; Harley, K. G.; Bradman, A.; Gharbi, M.; Sjodin, A.; Eskenazi, B. *Environ. Health Perspect.* **2010**, *118*, 1444.
(11) La Guardia, M. J.; Hale, R. C.; Harvey, E. *Environ. Sci. Technol.* **2006**, *40*, 6247.
(12) Lagalante, A.; Oswald, T. *Anal. Bioanal. Chem.* **2008**, *391*, 2249.
(13) Alaee, M.; Sergeant, D.; Ikonomou, M.; Luross, J. *Chemosphere* **2001**, *44*, 1489.
(14) Covaci, A.; Voorspoels, S.; de Boer, J. *Environ. Int.* **2003**, *29*, 735.
(15) Gosavi, R. A.; Knudsen, G. A.; Birnbaum, L. S.; Pedersen, L. C. *Environ. Health Perspect.* **2013**, *121*, 1194.
(16) Ding, N.; Chen, X. F.; Wu, C. M. L. *Environ. Sci.: Nano* **2014**, *1*, 55.
(17) Jaworski, J. W.; Raorane, D.; Huh, J. H.; Majumdar, A.; Lee, S.-W. *Langmuir* **2008**, *24*, 4938.
(18) Oh, J. W.; Chung, W. J.; Heo, K.; Jin, H. E.; Lee, B. Y.; Wang, E.; Zueger, C.; Wong, W.; Meyer, J.; Kim, C.; Lee, S. Y.; Kim, W. G.; Zemla, M.; Auer, M.; Hexemer, A.; Lee, S. W. *Nat. Commun.* **2014**, *5*, 3043.
(19) Savory, N.; Abe, K.; Sode, K.; Ikebukuro, K. *Biosens. Bioelectron.* **2010**, *26*, 1386.
(20) Jaworski, J.; Yokoyama, K.; Zueger, C.; Chung, W.-J.; Lee, S.-W.; Majumdar, A. *Langmuir* **2011**, *27*, 3180.
(21) Weiss, G. A.; Watanabe, C. K.; Zhong, A.; Goddard, A.; Sidhu, S. S. *Proc. Natl. Acad. Sci. U. S. A.* **2000**, *97*, 8950.
(22) Kim, T. H.; Lee, B. Y.; Jaworski, J.; Yokoyama, K.; Chung, W.-J.; Wang, E.; Hong, S.; Majumdar, A.; Lee, S.-W. *ACS Nano* **2011**, *5*, 2824.
(23) Lee, B. Y.; Sung, M. G.; Lee, J.; Baik, K. Y.; Kwon, Y.-K.; Lee, M.-S.; Hong, S. *ACS Nano* **2011**, *5*, 4373.
(24) Zhou, X.; Moran-Mirabal, J. M.; Craighead, H. G.; McEuen, P. L. *Nat. Nanotechnol.* **2007**, *2*, 185.
(25) Kim, J.-M.; Lee, Y. B.; Yang, D. H.; Lee, J.-S.; Lee, G. S.; Ahn, D. J. *J. Am. Chem. Soc.* **2005**, *127*, 17580.
(26) Lee, R. S.; Kim, H. J.; Fischer, J. E.; Thess, A.; Smalley, R. E. *Nature* **1997**, *388*, 255.
(27) Masuko, T.; Minami, A.; Iwasaki, N.; Majima, T.; Nishimura, S.-I.; Lee, Y. C. *Biomacromolecules* **2005**, *6*, 880.
(28) Llorca-Porcel, J.; Martínez-Sánchez, G.; Álvarez, B.; Cobollo, M. A.; Valor, I. *Anal. Chim. Acta* **2006**, *569*, 113.
(29) Fontanals, N.; Barri, T.; Bergström, S.; Jönsson, J.-Å. *Journal of Chromatography A* **2006**, *1133*, 41.
(30) Hoh, E.; Hites, R. A. *Environ. Sci. Technol.* **2005**, *39*, 7794.

DOI: 10.1021/acs.nanolett.5b03678
Nano Lett. XXXX, XXX, XXX−XXX